1 Pressure correction

1.1 Failure of the Internal Pressure Sensor

The Li-820 maintains a stable cell temperature and corrects the absorptance of CO_2 based on a measurement of the pressure in the cell. During the cruise in August 2016, a failure of the internal pressure sensor occurred on August 25, 2016 at 22:53 GMT. The failure was evident, because the cell pressure reading dropped from a relatively stable value of 102 kPa to 62.57 kPa within 10 seconds. Even when all tubes and pumps were removed and the Li-820 cell pressure was allowed to adjust to ambient pressure, the reading did not change. The internal pressure correction that the Li-820 performs was thus based on the false reading of a cell pressure of 62.57 kPa. The setup had not been changed, and the cell pressure before the failure had been at a stable level of approximately 102.2 kPa. Consequently, the pressure correction done by the Li-820 was reversed and performed again assuming an internal cell pressure of 102.2 kPa for the time after the failure of the pressure sensor.

1.2 Pressure Correction in the Li-820

The CO_2 mole fraction in the Li-820 is computed from a pressure-corrected measurement of absorptance. The pressure correction is performed by multiplication of the absorptance α_c with an empirically determined correction function (Li-820 Manual, Eq. 4-4):

$$\alpha_{pc} = \alpha_c g_c(\alpha_c, P) \tag{1}$$

$$g_c(\alpha_c, P) = \begin{cases} X for P < P_0 \\ 1 for P = P_0 \\ \frac{1}{X} for P > P_0 \end{cases} \tag{2}$$

with $P_0 = 99kPa$ and $X = \frac{1}{\frac{1}{b_1(p-1)} + \frac{(\frac{1}{b_5-\alpha_c} - \frac{1}{b_5})}{\frac{1}{b_2+b_3 p} + b_4}} + 1$ (Li-820 manual, Eq. 4-6). In this equation, $p = \frac{P_0}{P}$ or $\frac{P}{P_0}$, with $p > 1$.

So

$$\alpha_{pc} = \begin{cases} \alpha_c \cdot X for P < P_0 \\ \frac{\alpha_c}{X} for P > P_0 \\ \alpha_c for P = P_0 \end{cases} \tag{3}$$

1.3 Correction for false cell pressure

In order to correct for the false cell pressure P_{meas}, the absorptance α_c has to be computed. Then, the pressure-corrected absorptance α_{pc} has to be calculated using the corrected pressure P_c. P_c was taken to be the average cell pressure during the measurements before the pressure sensor failed, which was 102.18

kPa. This value was considered a good approximation, as the cell pressure in the Li-820 was fairly stable during the time of measurements while the pressure sensor was still functioning.

The inverse function which allows calculation of the pressure-corrected absorptance from the mole fraction is given as

$$\alpha_{pc} = \frac{a_1 C}{a_2 + C} + \frac{a_3 C}{a_4 + C} \tag{4}$$

with $a_1 = 0.3989974$, $a_2 = 5897.2804$, $a_3 = 0.097101982$, $a_4 = 596.49981$ (Li-820 Manual, Eq. 4-7).

In order to calculate the absorptance α_c from α_{pc}, Equation 3 has to be rearranged and solved for α_c. The solutions are:

$$\alpha_c = \begin{cases} -\frac{P_1}{2} - \sqrt{(\frac{P_1}{2})^2 - Q_1} for P < P_0 \\ -\frac{P_2}{2} - \sqrt{(\frac{P_2}{2})^2 - Q_2} for P > P_0 \\ \alpha_c \end{cases} \tag{5}$$

whereas
$P_1 = \frac{\alpha_{pc} m b_5 (n+b_4) - \alpha_{pc} + b_5^2 (n+b_4)(m+1)}{-b_5 (n+b_4)(m+1)+1}$
$Q_1 = -\frac{\alpha_{pc} m b_5^2 (n+b4)}{-b_5 (n+b_4)(m+1)+1}$
$P_2 = \frac{b_5^2 m (n+b_4) - \alpha_{pc} + \alpha_{pc} b_5 (1+m)(n+b_4)}{1 - b_5 m (n+b_4)}$
$Q_2 = -\frac{\alpha_{pc} b_5^2 (1+m)(n+b_4)}{1 - b_5 m (n+b4)}$
with $m = \frac{1}{b_1 (p-1)}$ and $n = \frac{1}{b_2 + b_3 p}$.

From α_c and P_c, the corrected $\alpha_{pc,c}$ is calculated according to Equation 1. C_c is calculated according to the manual:

$$C_c = \frac{D - (a_2 + a_4)\alpha_{pc,c} - \sqrt{A^2 \alpha_{pc,c}^2 + B \alpha_{pc,c} + D^2}}{2(\alpha_{pc,c} - a_1 - a_3)} \tag{6}$$

whereas $A = a_2 - a_4$, $B = 2A(a_1 a_4 - a_2 a_3)$ and $D = a_3 a_2 + a_1 a_4$ (Li-820 Manual, Eq. 4-10 and 4-11).

2 Salinity Interpolation

Salinity was only available at the stations (15 in the wet season, 34 in the dry season). However, in order to be able to interpret O_2 and CO_2 data, it is useful to know their distribution along a salinity gradient. Therefore, salinity in the estuary was spatially interpolated. Since the saltwater intrusion limit was presumably different between wet and dry season, interpolation was performed for the entire area under tidal influence (downstream of Kanowit). Beyond that point, salinity was measured to be zero.

Since some points for which interpolation was desired lay outside the area covered by our measurements, we added three reference points to better constrain the grid to be interpolated. The coordinates of these points were:

$$(2.0, 2.5, 3.5), (111.0, 111.0, 111.8) \tag{7}$$

These reference points all lie within the South China Sea off the coast of Sarawak. The salinity value ascribed to them was 33 according to our own measurements and those of Wang et al. (2014) for the Southern South China Sea. Interpolation was achieved with the Scipy Interpolation package for Python (scipy.interpolate.griddata) using linear interpolation. Figure 1a shows the points used for interpolation, Figures 1b and c show the results for the wet and dry season, respectively.

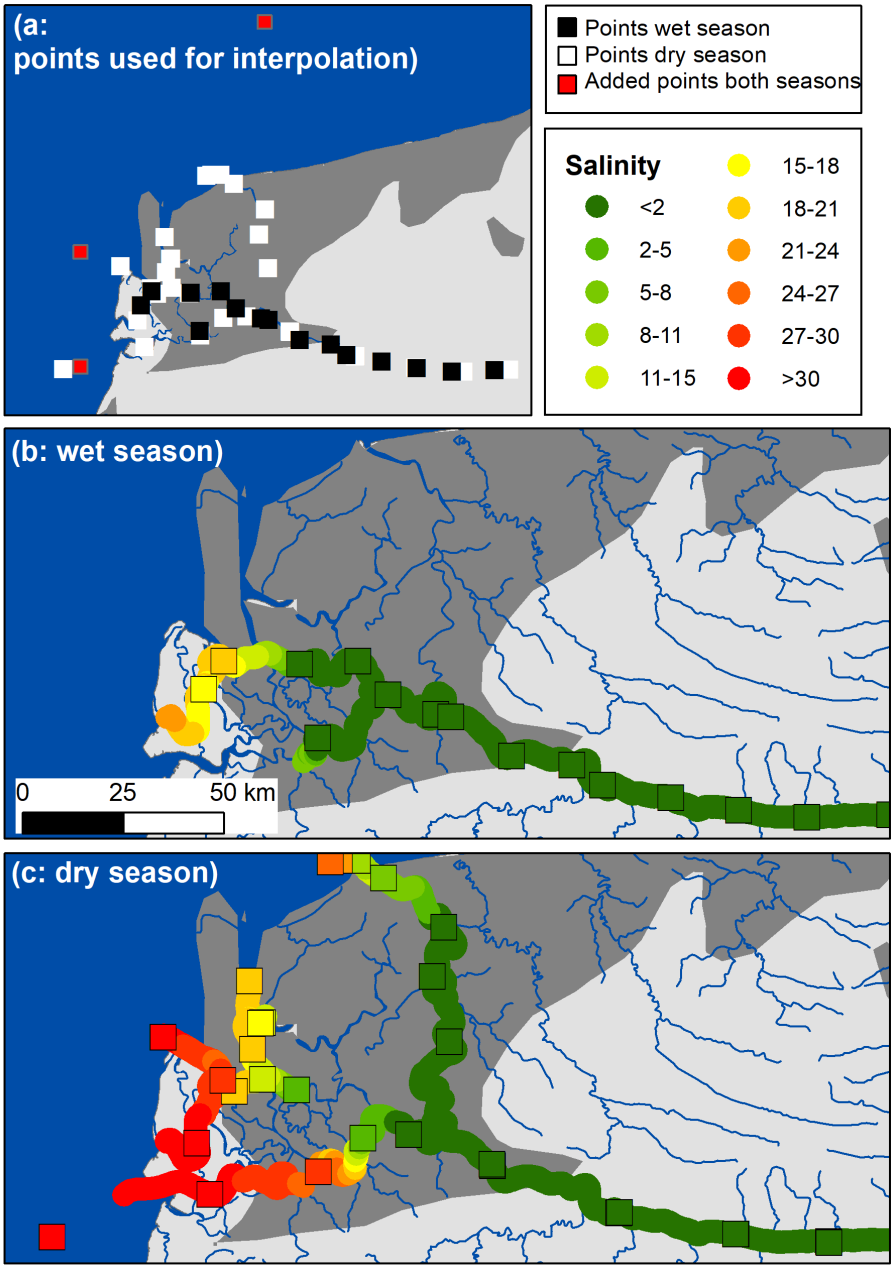

Figure 1: Data points used for interpolation (a), results for the wet (b) and dry (c) season. Interpolated salinity is shown in graduated colors, actual measurements are shown as squares.

3 Water surface area in the delta

Similar to Müller et al. (2016), we used the water surface areas for Malaysia as estuarine surface area (obtained at http://www.diva-gis.org/). However, the shapefiles only contain part of the Rajang River and Delta, so missing parts were manually delineated using a georeferenced satellite image (Fig. 2). Water surface areas were added. For the two seasons, salinity intrusion was estimated from interpolated salinity, and the water surface area was calculated for both the saline (=estuary) and the freshwater part (=peat) of the delta. The corresponding water surface areas for the peat area are displayed in Figure 2b and c. The estuarine surface area was then calculated from the entire water surface area in the delta minus the peat area.

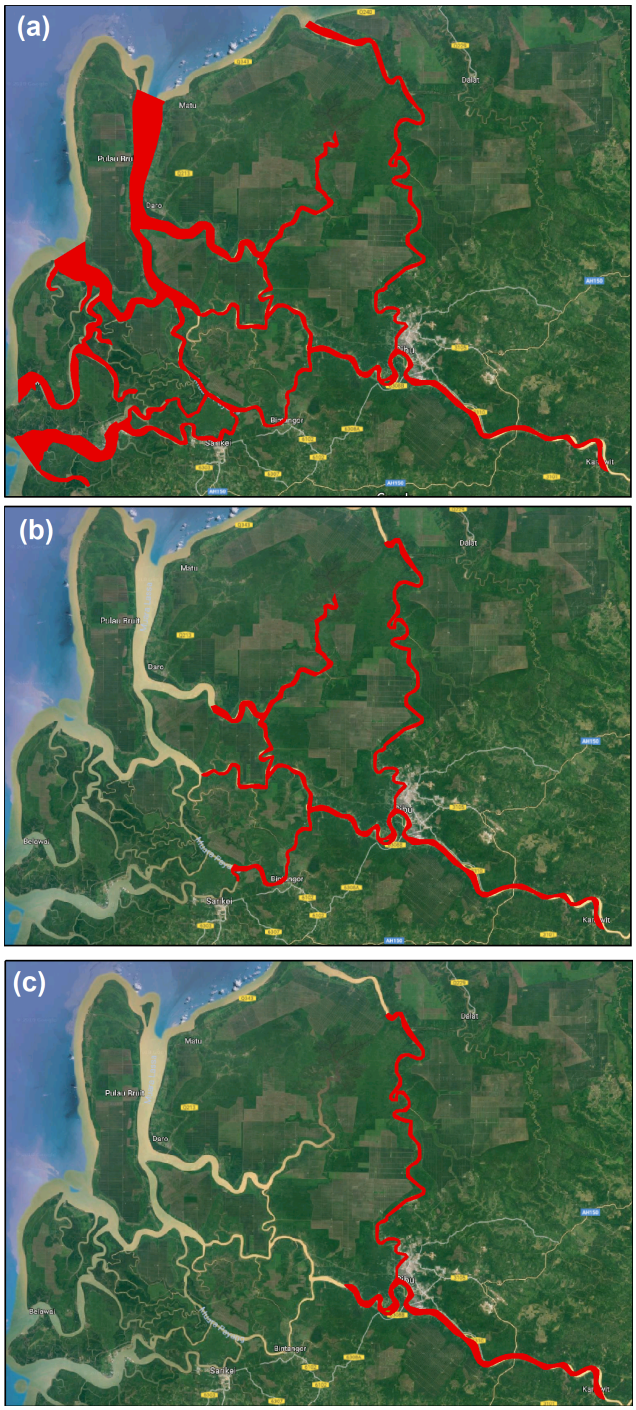

Figure 2: Water surface area estimated for the entire Rajang delta (a), water surface area in the peat area during the wet (b) and dry (c) season.

4 Comparison of different k-models

Table 1 presents a comparison of three different k-parameterizations.

	k_{600}			FCO_2		
	B04	A11	R01	B04	A11	R01
wet	8.23	8.51	2.32	2.28 ± 0.52	2.36 ± 0.54	0.64 ± 0.15
dry	9.57	12.19	2.79	2.45 ± 0.45	3.12 ± 0.58	0.71 ± 0.13

Table 1: Comparison of the results for different k-parameterizations. B04: Borges et al. (2004), A11: Alin et al. (2011), R01: Raymond & Cole (2001).

5 Mixing model

We used a simple mixing model to estimate the theoretically possible contribution of the peatlands to river pCO_2. The model consists of two subsequent steps. First, the mixing of two water bodies was simulated, one with a pCO_2 of 2434 μatm and a pH of 6.8 (Rajang River), and the other with a pCO_2 of 8100 μatm and a pH of 3.8 (representing peat-draining rivers according to Müller et al., 2015). The DIC and TA of these water bodies were calculated using CO_2Sys. DIC and TA of the mixture were calculated as

$$DIC_{S=0} = (1 - pc) \cdot DIC_1 + pc \cdot DIC_2 \tag{8}$$

and

$$TA_{S=0} = (1 - pc) \cdot TA_1 + pc \cdot TA_2, \tag{9}$$

whereas pc is the peat coverage in the basin as the river flows downstream and passes through more and more peat areas (pc=0...0.11). As a next step, for pc>0.03, mixing with saltwater was taken into account. It was assumed that pc=0.03 correpsonds to S=0 and that pc=0.11 corresponds to S=32 and within this range, salinity increased linearly with increasing peat coverage. This is obviously a simplification, but since the model has only illustrative purposes, it seemed sufficient. DIC and TA were then calculated with a normal end-member mixing model:

$$DIC = \frac{DIC_{S=32} - DIC_{S=0}}{32} \cdot S + DIC_{S=0} \tag{10}$$

and

$$TA = \frac{TA_{S=32} - TA_{S=0}}{32} \cdot S + TA_{S=0}, \tag{11}$$

whereas $TA_{S=32} = 2324 \mu mol L^{-1}$ and$DIC_{S=32} = 2347 \mu mol L^{-1}$ according to our measurements. pCO_2 was calculated from TA and DIC using CO_2Sys. The mixing model and the results are shown in Figure 3.

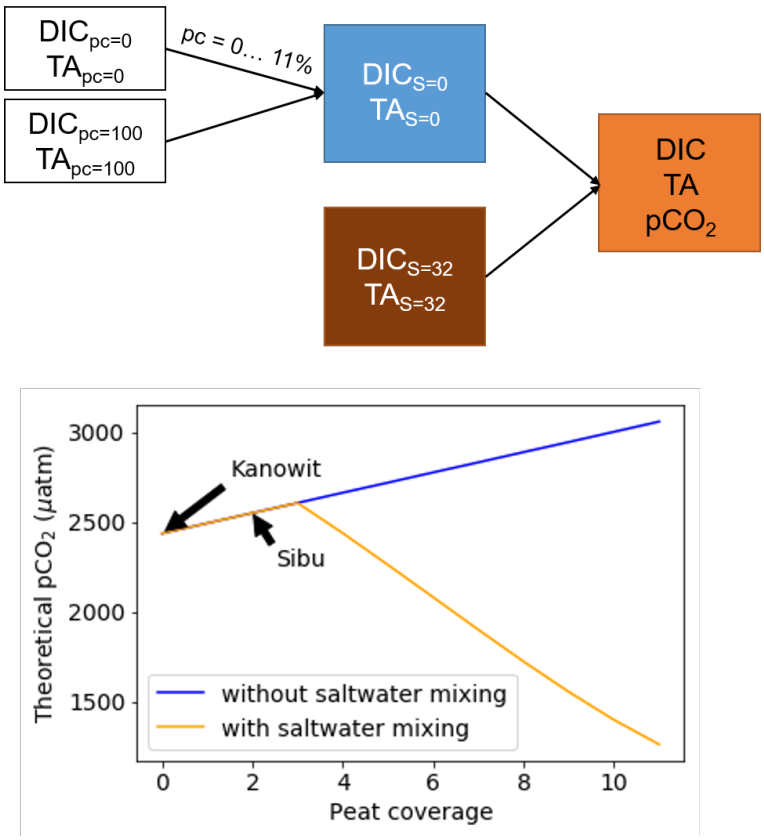

Figure 3: Mixing model flow chart and plot of the results for theoretically possible pCO_2 if peat is the only source of CO_2 in the delta.

6 Supplementary Data

The data used in this manuscript are available as a separate excel workbook.

7 References

Alin, S. R., de Fatima F. L. Rasera, M., Salimon, C., I., Richey, J. E., Holtgrieve, G. W., Krusche A. V., and Snidvongs, A. Physical controls on carbon dioxide transfer velocity and flux in low-gradient river systems and implications for regional carbon budgets. Journal of Geophysical Research 116, G01009, doi: 10.1029/2010JG001398, 2011.

Borges, A. V., Vanderborght, J.-P., Schiettecatte, L.-S., Gazeau, F., Ferron-Smith, S., Delille, B., and Frankignoulle, M. Variability of the Gas Transfer

Velocity of CO2 in a Macrotidal Estuary (the Scheldt). Estuaries 27(4): 593-603, 2004.

LI-COR, Inc. Li-820 Instruction Manual, Lincoln, Nebraska, USA, 2002.

Müller, D., Warneke, T., Rixen, T., Müller, M., Jamahari, S., Denise, N., Mujahid, A., and Notholt, J. Lateral carbon fluxes and CO2 outgassing from a tropical peat-draining river. Biogeosciences 12: 5967-5979. doi: 10.5194/bg-12-5967-2015, 2015.

Müller, D., Warneke, T., Rixen, T., Müller, M., Mujahid, A., Bange, H. W., and Notholt, J. Fate of terrestrial organic carbon and associated CO2 and CO emissions from two Southeast Asian estuaries. Biogeosciences 13: 691-705. doi: 10.5194/bg-13-691-2016, 2016.

Raymond, P. A., and Cole, J. J. Gas exchange in rivers and estuaries: Choosing a gas transfer velocity. Estuaries 24 (2): 312-317, 2001.

Wang, Y., Jiang, H., Zhang, X., and Jin, J. Spatial and temporal distribution of sea surface salinity in coastal waters of China based on Aquarius. IOP Conference Series: Earth and Environmental Science 17: 012116, 2014.